Superradiant Smith-Purcell Emission

J. Urata, M. Goldstein,* M. F. Kimmitt,† A. Naumov, C. Platt, and J. E. Walsh
Department of Physics and Astronomy, Dartmouth College, Hanover, New Hampshire 03755-3528
(Received 2 July 1997)

A diffraction grating mounted in the electron beam focal region of a scanning electron microscope has been used to produce superradiant emission over the 300–900 μm wavelength range. Feedback is provided by the grating itself and the electron beam is focused and positioned over the grating by the microscope's electron optical system. Extensions of this technique promise a new tunable, coherent, cw source for the difficult to access far infrared (30–1000 μm) range of the spectrum. [S0031-9007(97)05020-5]

PACS numbers: 41.60.–m, 07.57.Hm, 52.75.Ms

This Letter contains a description of a new type of grating-based, tunable source that operates in the far-infrared (FIR) region of the spectrum. Superradiant emission is achieved using a low energy spread, low emittance ("bright") electron beam, and a diffraction grating. Distributed feedback is provided by the grating itself. The device, which is described as a grating coupled oscillator (GCO), has the potential for operating over the entire, difficult to access, FIR (30–1000 μm) region of the spectrum.

A traditional means of pushing the operating regime of electron beam driven, coherent radiation sources toward significantly shorter wavelengths has been to move the electron beam energy into the relativistic regime. The present results provide clear evidence that significant decreases in beam energy spread and emittance, i.e., improvements in beam quality, can also be used for this purpose. This observation applies equally to the broad class of beam-field coupling schemes and not just the diffraction gratings used in the present Letter.

When an electron passes close to the surface of a metal diffraction grating, radiation is produced at wavelengths that can be determined from the expression

$$\lambda = \frac{l}{|n|}\left(\frac{1}{\beta} - \sin\theta\right). \quad (1)$$

In Eq. (1) l is the grating period, $\beta \equiv v/c$ is the electron velocity relative to the speed of light (c), θ is the angle of emission measured from a direction normal to the surface of the grating, and n is the spectral order. Light produced in this manner was first observed by Smith and Purcell [1], and it has come to be known as Smith-Purcell radiation.

The original work of Smith and Purcell was carried out at visible wavelengths as were a number of subsequent investigations [2,3]. The effect of the stimulated component of the emission process was negligible in these experiments. At long (mm) wavelengths devices based on gratings have been operated as coherent oscillators, but in order to achieve threshold, feedback elements have been required [4,5]. In the present case the distributed feedback on the grating is used for this purpose. The grating serves as both the coupling element and the resonator. A substantial fraction of the energy transferred from the beam to the field is presumed to be in the form of nonradiative space harmonics and external feedback elements are not required. In principle, however, their use may provide additional flexibility in the design. The open surface resonator together with the high quality electron beam facilitates operation in the FIR wavelength range.

The device uses the beam of a scanning electron microscope (SEM), a schematic of which is shown in Fig. 1. The SEM is capable of generating a continuous, cylindrical, 20–40 keV, a $\geq$20 μm (waist) diameter beam with a total current $\leq$1 mA. The energy spread is not measured directly but it is presumed to be small given the design parameters of the electron microscope. Emittance is measured using a 500 μm slit. It is typically in the range of 2×10^{-2} π mm mrad in the present system and varies by less than a factor of 2 over the range of current used in these experiments. A rectangular grating profile was chosen, and the theory of van den Berg [6] was used to determine the grating dimensions that maximize the power of first order spontaneous radiation ($n = -1$) at $\theta = 0$.

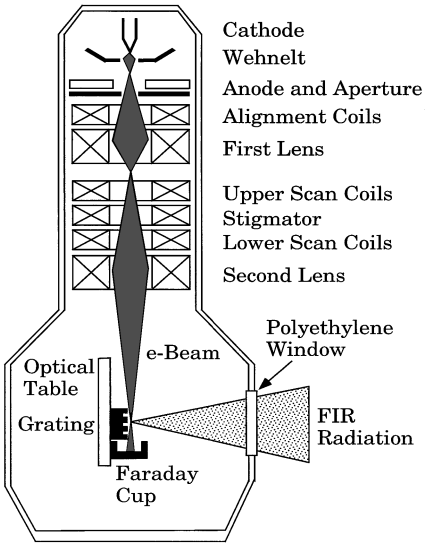

FIG. 1. Schematic of the modified SEM.

 0031-9007/98/80(3)/516(4)$15.00

The gratings that were used ranged in period from 128 to 308 μm.

The angular distribution of the power (W/sr) radiated into the half-space above the grating (see Fig. 2) by a beam of uncorrelated electrons in the spontaneous emission limit is given by [7]

$$\frac{dP}{d\Omega} = \frac{INen^2\beta^3}{2l\epsilon_0}\,\frac{\cos^2\theta\cos^2\phi}{(1-\beta\sin\theta)^3}\,|R_n(\theta,\phi,\beta,s/l,d/l)|^2 \times \exp\left[\frac{-4\pi|n|y_0\sqrt{1+\gamma^2\beta^2\cos^2\theta\sin^2\phi}}{\gamma l(1-\beta\sin\theta)}\right], \tag{2}$$

where I is the beam current, e is the electron charge, N is the number of grating periods, ϵ_0 is the permittivity of free space, y_0 is the beam's impact parameter, ϕ is the azimuthal angle from the y axis, and $\gamma \equiv (1-\beta^2)^{-\frac{1}{2}}$.

The factor $|R_n|^2$ is related to the grating efficiency and describes how well a grating of a specific geometry radiates at a particular beam energy. The modal expansion method of van den Berg [6] was used to calculate $|R_n|^2$. The value of $|R_1|^2$ at 35 kV in the normal direction is 3.4 for the grating used. In this model the near field associated with a moving electron is incident on the grating where it diffracts into radiating and nonradiating orders. The nonradiating orders are evanescent surface waves which have phase velocities less than the speed of light. When one of these "slow" waves has a phase velocity close to the velocity of an electron, the electron can transfer energy to the wave and thereby indirectly drive the radiating orders. This is the basic beam-field coupling mechanism in both the spontaneous and superradiant regimes.

Effective coupling occurs when the beam is within the synchronous slow wave's $1/e$ length. Equation (1) and the velocity matching of the beam and the space harmonic can be used to calculate the evanescent scale. At resonance, for emission in the $\phi = 0$ plane, the scale length is determined by $\lambda_c = \lambda\beta\gamma/4\pi$. Equation (2) is derived using a delta function beam and is a good approximation of the spectral radiance if the actual beam diameter is small compared with λ_c. If this is not the case then an integration over the beam's transverse distribution is performed.

In the experiments the beam waist was placed at the midpoint of the grating, and the SEM's scanning coils were used to sweep the beam perpendicular to the surface of the grating at 200 Hz. This created a reference modulation on the signal. The power was directed out of the SEM through a polyethylene window and either focused into a Czerny-Turner monochromater or collimated into a Michelson interferometer. A helium-cooled, silicon composite bolometer was used for detection.

The wavelengths corresponding to the peak signals through the monochromater are in excellent agreement with those predicted by Eq. (1) (Fig. 3). In addition, a wire grid polarizer was used to confirm that the radiation is strongly polarized (Fig. 4).

The time averaged power incident on the detector was recorded as a function of beam current. In the limit where spontaneous emission dominates, the power

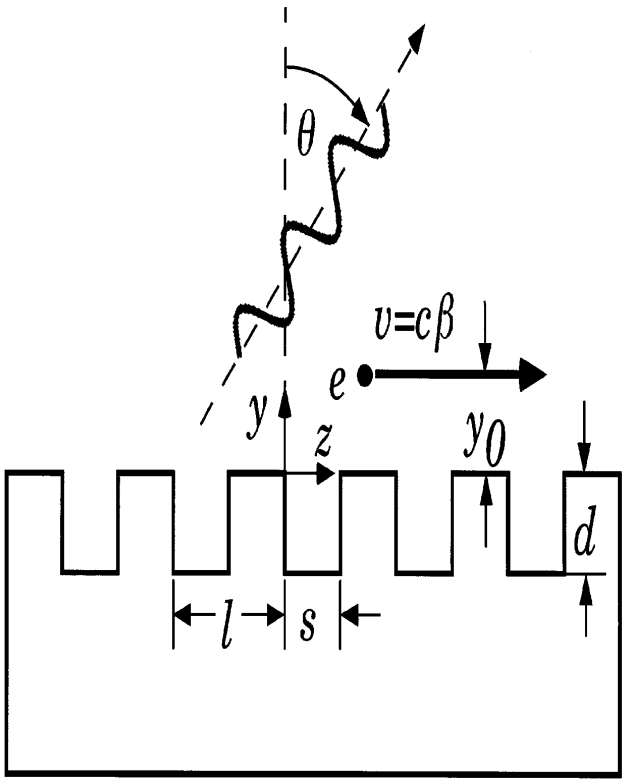

FIG. 2. Diagram showing the coordinate system and parameters. Grating dimensions, in microns, for the data displayed in Fig. 5 are $l = 173, s = 62, d = 100$, and the grating length L is 12.7 mm (73 periods).

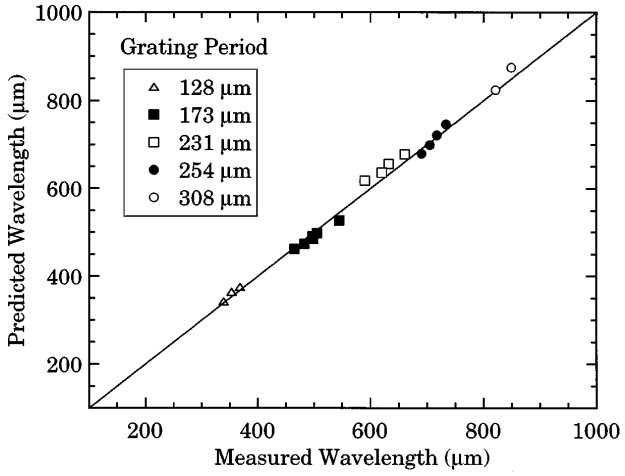

FIG. 3. Theoretically predicted vs experimentally measured wavelength for gratings of various periods run at beam energies between 30 and 40 keV (error bars are approximately the same size as the data points).

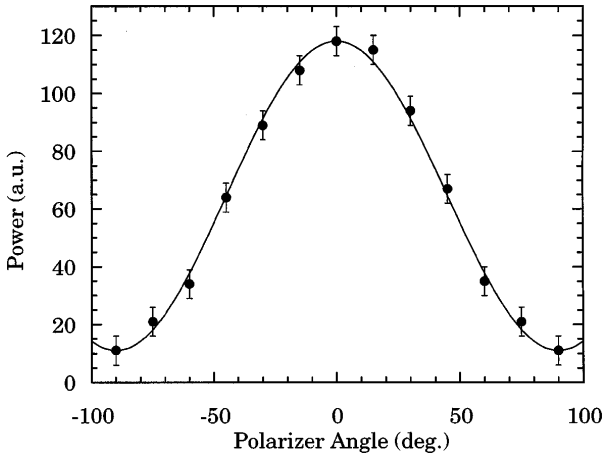

FIG. 4. Detected power vs polarizer angle using the $l = 173$ μm grating with a beam current of 100 μA at 35 keV.

increases linearly with the beam current [see Fig. 5 and Eq. (2)]. When the beam current surpasses a certain threshold, however, the detected power evolves from a linear to a superlinear current dependence. There was no discernible difference in the light's polarization or wavelength between the two regimes. The transition from a linear to a superlinear dependence of the power on the beam current indicates the onset of a stimulated process. In the example shown in Fig. 5, power rises as the fourth power of the beam current. The log-log plots of power versus current always have a slope of one below threshold and show a straight line behavior above the transition point. The quartic dependence does not appear to be universal; small changes in beam focus have yielded slopes ranging from 3 to 6. The higher slopes are generally associated with higher start currents and may be a consequence of a small change in the effective

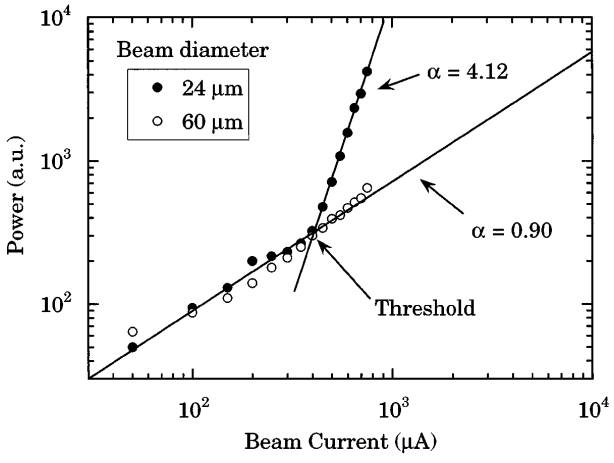

FIG. 5. Detected power vs electron beam current using the $l = 173$ μm grating for two electron beam diameters at 35 keV. Fits were made of the form $y = Ax^{\alpha}$. The threshold point for the smaller diameter beam is indicated.

interaction length. The waist of the beam is nominally independent of beam current.

A detailed theory for the GCO, particularly one that addresses the optics of a grating that is functioning as a surface resonator, does not yet exist. However, the device is functionally a member of the traveling wave family, and this realization can be used to describe device performance in qualitative terms. The results of a set of measurements intended to illustrate this point are gathered together in Table I. These choices are inspired by general theories of traveling wave [8] and grating coupled devices [9].

First the threshold current was determined as the waist diameter of the beam was varied. As expected, larger diameter beams required more current to initiate the oscillation. The larger beams also reached threshold at a somewhat lower current density. This would be anticipated as well since the geometric filling factor will increase with beam diameter. The values of the start current and start current density are listed in the table.

Presuming that collective excitation on the electron beam will become evident near threshold, it is of interest to examine the beam plasma frequency. This parameter is defined by

$$\omega_p^2 = \frac{n_b e^2}{\epsilon_0 m \gamma^3}, \tag{3}$$

where n_b is the beam density. The factor γ^3 is included because it is presumed that it is the longitudinal mass that is important in the bunching. A single power of γ could be more appropriate but this is immaterial at the present energy. It is conveniently measured in units of the transit time τ of an electron through the interaction region. The values of $\omega_p \tau$ at threshold are listed in the table. It can be seen that threshold is reached when $\omega_p \tau$ is an appreciable fraction of unity.

When the GCO is operating on a single mode, energy transfer is dominated by resonant coupling with a single, synchronous space harmonic. In this case the space charge waves on the beam and the components of a particular space harmonic that is approximately synchronous with the beam are in effect a coupled three wave system. The structure of the coupling constant will thus have the general form [8,9]

$$\Delta_c \simeq \frac{\sqrt{3}}{2} (\omega_p^2 \omega \tau^3)^{1/3} f^{1/3}, \tag{4}$$

TABLE I. Summary of a series of superradiant threshold measurements. The first three columns are the beam waist diameter, the current at the superradiant emission threshold, and the waist current density at this point.

d_b (μm)	I_{st} (μA)	J_{st} (A/cm^2)	$\omega_p \tau$	$g_0/f^{1/3}$ (db)
24	450	99.47	1.17	59.6
36	550	54.03	0.865	48.7
44	600	39.46	0.740	43.9
60	800	28.29	0.626	39.3

where f is an unknown and presumably a small dimensionless coupling factor. The intrinsic forward gain for the local wave system in this case would be

$$g_0 = 47.3(\Delta_c/2\pi)\ (\mathrm{db})\,, \tag{5}$$

where the final expression has been cast in a form which emphasizes the relation with traveling wave interaction theory [8]. Values of $g_0/f^{1/3}$ are shown in the last column of the table.

It must be emphasized that Eq. (5) does not represent a net gain because it does not take into account the redistribution of the energy in the driven space harmonic among the full set of space harmonics, the intrinsic 9.54 db coupling loss [8], surface loss, or the loss due to the power radiated. The argument, however, does reveal the fact that the intrinsic gain available from low energy but high quality (low energy spread, low emittance) beams of modest total current is potentially very large. At currents above threshold, values of f no larger than 10^{-3}–10^{-2} would yield substantial net gain.

The power produced in the limit where spontaneous emission dominates is accurately given by Eq. (2) [10]. Recognizing that in the spontaneous limit Eq. (2) describes a shot noise process, a radiation resistance can be extracted by dividing out the factors e and I, integrating in the ϕ direction, and converting from $d\theta$ to either frequency or wave number intervals. The results of these manipulations are displayed in Fig. 6. The estimated peak radiation resistance for the 173 μm period grating is approximately 1.6 kΩ when the beam centroid is one beam radius above the grating. The factors multiplying the radiation resistance ($ceId\overline{\nu}$) combine to yield 4.8 fW/(μA cm^{-1} Ω). Thus in the spontaneous limit approximate power levels in the 8 pW/(μA cm^{-1}) range are expected. The values are in good agreement with the measured power levels (100's of pW) when the beam current is in the 100–200 μA (below threshold) regime.

Above threshold the degree of coherent modulation on the beam will be an implicit function of the radiation resistance. The theory for this evolution is not yet developed, but it is possible to estimate the magnitude of the coherent modulation using the measured power and the radiation resistance. At beam current values approximately a factor of 2 above threshold the power on the detector is a few 10's of nW. Measurements of the throughput of the optical system indicate that power levels in the μW range are available on the grating. This implies that $(\overline{\delta I_{\mathrm{coh}}^2})^{1/2}$ is of the order of 5% to 10% of the average current.

The power levels available are already sufficient to conduct spectroscopic experiments. Furthermore, since the present system operates with a tungsten "hairpin" cathode, modest improvements in the apparatus, particularly in the electron gun, are expected to yield a very useful laboratory based FIR radiation source. Given the progress in high brightness field emission cathode research [11] and the emerging capabilities of physically small dc-dc high voltage, low current power supplies, future development of compact portable versions of this device is also a realistic expectation.

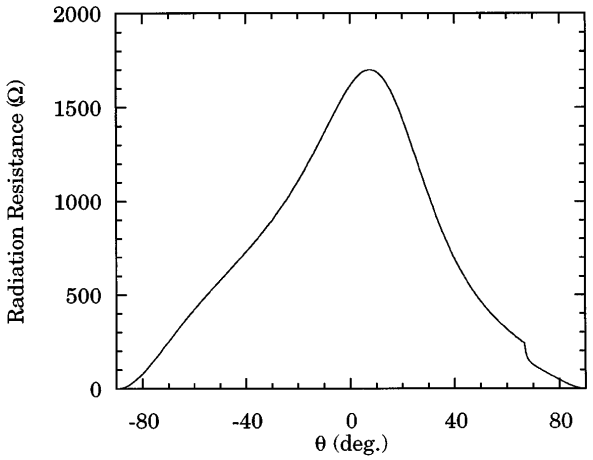

FIG. 6. Radiation resistance in ohms vs the angle of emission for the $l = 173$ μm grating when operated at 35 keV.

The authors would like to thank Vanderbilt University for the loan of the bolometer. The support of ARO Contract DAAH04-95-1-0640 and Vermont Photonics, Inc. is gratefully acknowledged.

*Present address: Intel Corporation, SC2-16, 2200 Mission College Blvd., Santa Clara, California 95052.
†Also affiliated with the Department of Physics, University of Essex, Colchester C04 3SQ, England.

[1] S. J. Smith and E. M. Purcell, Phys. Rev. **92**, 1069 (1953).
[2] E. L. Burdette and G. Hughes, Phys. Rev. A **14**, 1766 (1976).
[3] I. Shih *et al.*, Opt. Lett. **15**, 559 (1990).
[4] *Infrared and Millimeter Waves*, edited by K. J. Button (Academic Press, New York, 1979); see the chapters on the Ledatron (Vol. 1) and the Orotron (Vol. 7).
[5] J. Killoran, F. Hacker, and J. E. Walsh, IEEE Trans. Plasma Sci. **22**, 530 (1994).
[6] P. M. van den Berg and T. H. Tan, J. Opt. Soc. Am. **64**, 325 (1974).
[7] K. J. Woods *et al.*, Phys. Rev. Lett. **74**, 3808 (1995).
[8] J. R. Pierce, in *Traveling-Wave Tubes* (D. Van Nostrand Company, Inc., New York, 1950), pp. 13–16.
[9] L. Schachter and A. Ron, Phys. Rev. A **40**, 876 (1989).
[10] M. Goldstein *et al.*, Appl. Phys. Lett. (to be published).
[11] C. M. Tang, M. Goldstein, T. A. Swyden, and J. E. Walsh, Nucl. Instrum. Methods Phys. Res., Sect. A **358**, 7 (1995).